



## Data Article

# Experimental data on the removal of acid orange 10 dye from aqueous solutions using TiO<sub>2</sub>/Na-Y zeolite and BiVO<sub>4</sub>/Na-Y zeolite nanostructures: A comparison study



Behzad Rahimi<sup>a</sup>, Nayereh Rezaie-Rahimi<sup>b</sup>, Negar Jafari<sup>c,d</sup>,  
Ali Abdollahnejad<sup>e</sup>, Afshin Ebrahimi<sup>c,d,\*</sup>

<sup>a</sup> Student Research Committee, School of Health, Isfahan University of Medical Sciences, Isfahan, Iran

<sup>b</sup> Department of Health, Safety and Environment, Pasteur Institute of Iran, Tehran, Iran

<sup>c</sup> Environment Research Center, Research Institute for Primordial Prevention of Non-communicable Disease, Isfahan University of Medical Sciences, Isfahan, Iran

<sup>d</sup> Department of Environmental Health Engineering, School of Health, Isfahan University of Medical Sciences, Isfahan, Iran

<sup>e</sup> Department of Public Health, Maragheh University of Medical Sciences, Maragheh, Iran

## ARTICLE INFO

## Article history:

Received 16 December 2020

Revised 23 January 2021

Accepted 9 February 2021

Available online 12 February 2021

## Keywords:

Nanomaterials

TiO<sub>2</sub>/zeolite

BiVO<sub>4</sub>/zeolite

Acid orange 10

Dye degradation

## ABSTRACT

The increase of textile factories, along with the continuous development of industrialization has led to excessive discharge of high toxicity wastewater along with a diverse range of contaminants in wastewater. In this regard, to reduce their operating costs and treatment time, in this work, two synthesized nanostructures, TiO<sub>2</sub>/Na-Y zeolite and BiVO<sub>4</sub>/Na-Y zeolite was compared to remove acid orange 10 (AO10) from the aqueous solutions. The obtained optimum operating conditions including initial dye concentration, initial pH, contact time, catalyst dosage and AO10 removal efficiency were 20 mg/L, 3, 7 min, 0.2 g/100 mL, and 99.77% for TiO<sub>2</sub>/Na-Y zeolite and 20 mg/L, 3, 200 min, 0.2 g/100 mL and 46.13% for BiVO<sub>4</sub>/Na-Y zeolite composite, respectively. The structural characteristics of the synthesized materials were also determined by X-ray diffraction (XRD), field emission scanning

\* Corresponding author at: Environment Research Center, Research Institute for Primordial Prevention of Non-communicable Disease, Isfahan University of Medical Sciences, Isfahan, Iran.

E-mail address: [a\\_ebrahimi@hlth.mui.ac.ir](mailto:a_ebrahimi@hlth.mui.ac.ir) (A. Ebrahimi).

electron microscopy (FESEM), and fourier-transform infrared spectroscopy (FTIR).

© 2021 The Authors. Published by Elsevier Inc.

This is an open access article under the CC BY license (<http://creativecommons.org/licenses/by/4.0/>)

## Specifications Table

Subject	Environmental Chemistry
Specific subject area	Adsorption
Type of data	Table, image, and figure
How data was acquired	The initial and final AO10 concentration was analyzed by measuring its maximum absorbance ( $\lambda_{\text{max}} = 475 \text{ nm}$ ) using a DR-5000, HACH LANGE, USA spectrophotometer. The crystal structure analysis of the nanomaterials was detected via XRD device. The morphology observation was also detected by a field-emission scanning electron microscope (FE-SEM, the MIRA3 model, developed by TESCAN Company). Fourier transform infrared spectra (FTIR) was analyzed by Tensor 27-Equinox 55 model, Bruker corporation. RSM was employed to evaluate the main interaction effects and to optimize the number of nanomaterial process experiments using the Design-Expert 11.0.1 software.
Data format	Raw, Analyzed
Parameters for data collection	XRD device, Bruker Corporation (Germany) using a lamp Cu K $\alpha$ with a wavelength equal to 1.7890 Å at 40 kV and 40 mA, in the range of $2\theta = (10 \text{ to } 90)^\circ$ . A field-emission scanning electron microscope (FESEM), the MIRA3 model, developed by TESCAN company, operating voltage = 15 kV. The fourier transform infrared spectroscopy (FTIR) was in the range of 400–4000 $\text{cm}^{-1}$ with a resolution of 4 $\text{cm}^{-1}$ .
Description of data collection	Degradation of acid orange 10 by TiO <sub>2</sub> /Na-Y zeolite and BiVO <sub>4</sub> /Na-Y zeolite composite
Data source location	Isfahan University of Medical Sciences, Isfahan, Iran
Data accessibility	Data are available in this article
Related research article	A. Ebrahimi, N. Jafari, K. Ebrahimpour, A. Nikoonahad, A. Mohammadi, F. Fanaei, A. Abdolahnejad The performance of TiO <sub>2</sub> /NaY-zeolite nanocomposite in photocatalytic degradation of Microcystin-LR from aqueous solutions: Optimization by response surface methodology (RSM) Environmental Health Engineering and Management Journal <a href="http://10.34172/EHEM.2020.29">http://10.34172/EHEM.2020.29</a>

## Value of the Data

- TiO<sub>2</sub>/zeolite and BiVO<sub>4</sub>/zeolite composites which were synthesized by hydrothermal method, would be useful for the removal of toxic pollutants such as acid orange 10(AO10) dye from water and wastewater.
- These data show the better removal efficacy of TiO<sub>2</sub>/zeolite composite compared to BiVO<sub>4</sub>/zeolite composite on acid orange 10 removal.
- Process optimization using response surface methodology (RSM) by TiO<sub>2</sub>/zeolite and BiVO<sub>4</sub>/zeolite composites for dye removal yielded 99.77% and 46.13%, respectively.

## 1. Data Description

The presented data described the removal of acid orange 10 (AO10) dye by TiO<sub>2</sub>/zeolite and BiVO<sub>4</sub>/zeolite composites. The XRD pattern of TiO<sub>2</sub>/zeolite, TiO<sub>2</sub>, zeolite, BiVO<sub>4</sub>/zeolite, and

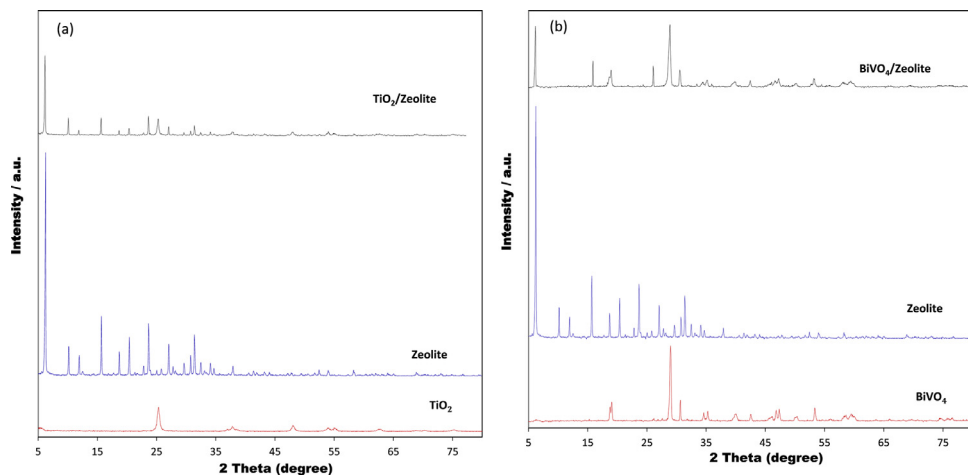


**Fig. 1.** The XRD pattern of the studied materials: a)  $\text{TiO}_2/\text{Zeolite}$ ,  $\text{TiO}_2$ , Zeolite; b)  $\text{BiVO}_4/\text{Zeolite}$ ,  $\text{BiVO}_4$ , Zeolite.

**Table 1**

Chemical properties of the AO10.

Chemical name	Acid Orange 10
Molecular weight (g/mol)	452.36
Maximum wavelength	475 nm
Structure	
Formula	$\text{C}_{16}\text{H}_{10}\text{N}_2\text{Na}_2\text{O}_7\text{S}_2$

$\text{BiVO}_4$  are presented in Fig. 1. The sharp peaks of anatase  $\text{TiO}_2$  are placed at  $2\theta$  of  $25.35^\circ$ ,  $37.8^\circ$ ,  $48.05^\circ$ ,  $54.95^\circ$ ,  $55.05^\circ$ , and  $62.55^\circ$  and for  $\text{BiVO}_4$  are displayed at  $2\theta$  of  $19.05^\circ$ ,  $29^\circ$ ,  $35.3^\circ$ , and  $47.35^\circ$  indicating successful synthesis of  $\text{BiVO}_4$  nanoparticle. Also, all the identified dominant peaks at  $2\theta$  belong to different minerals including Na, Al, and Si present in the XRD pattern of Na-Y zeolite with  $\text{Na}_5\text{Al}_6\text{Si}_{30}\text{O}_{72} \cdot 18\text{H}_2\text{O}$  formula. Fig. 1 also demonstrates the presence of Ti and Bi phase in Na-Y zeolite structure, while in the XRD pattern of Na-Y zeolite, these phases are not observed, indicating the successful coupling of  $\text{TiO}_2$  and  $\text{BiVO}_4$  to Na-Y zeolite structure. These results indicate that bismuth vanadate and titanium dioxide were not destroyed during the synthesis preparation process. The FE-SEM images of nanomaterials are illustrated in Fig. 2. The FTIR pattern of the studied materials is also represented in Fig. 3. Figs. 4 and 5 show the results of various factors in the form of three-dimensional surface plots on AO10 degradation efficiency for  $\text{TiO}_2/\text{zeolite}$  and  $\text{BiVO}_4/\text{zeolite}$ , respectively. Adsorption isotherms for AO10 removal on  $\text{TiO}_2/\text{zeolite}$  and  $\text{BiVO}_4/\text{zeolite}$  composite are presented in Figs. 6 and 7, respectively. Pseudo-second order kinetics for AO10 dye removal by  $\text{TiO}_2/\text{zeolite}$  and  $\text{BiVO}_4/\text{zeolite}$  are shown in Fig. 8. Figs. 9–12 illustrate the effects of nanomaterial dosage and pH on dye removal by the two studied nanostructures.

Specification of the AO10 is presented in Table 1. The properties of the Na-Y zeolite technical sheet are represented in Table 2. Tables 3 and 4 illustrate studied variables and ranges for AO10 dye removal by  $\text{TiO}_2/\text{zeolite}$  and  $\text{BiVO}_4/\text{zeolite}$ , respectively, based on the Design-Expert 11.0.1

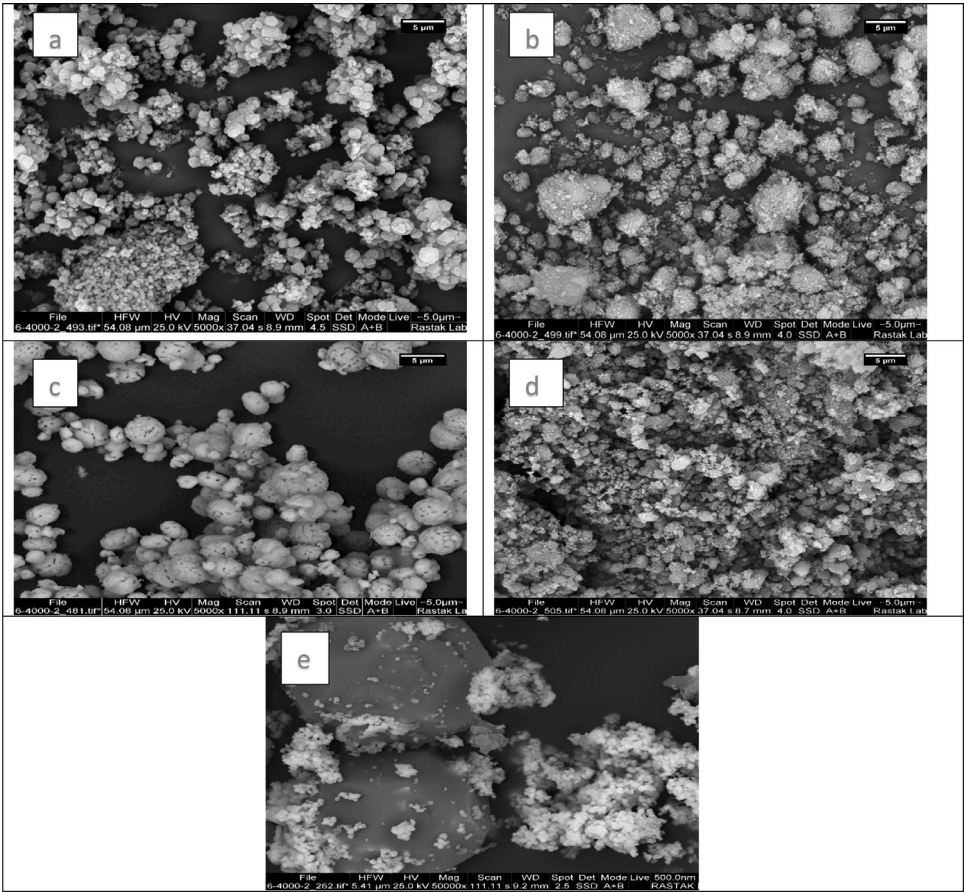
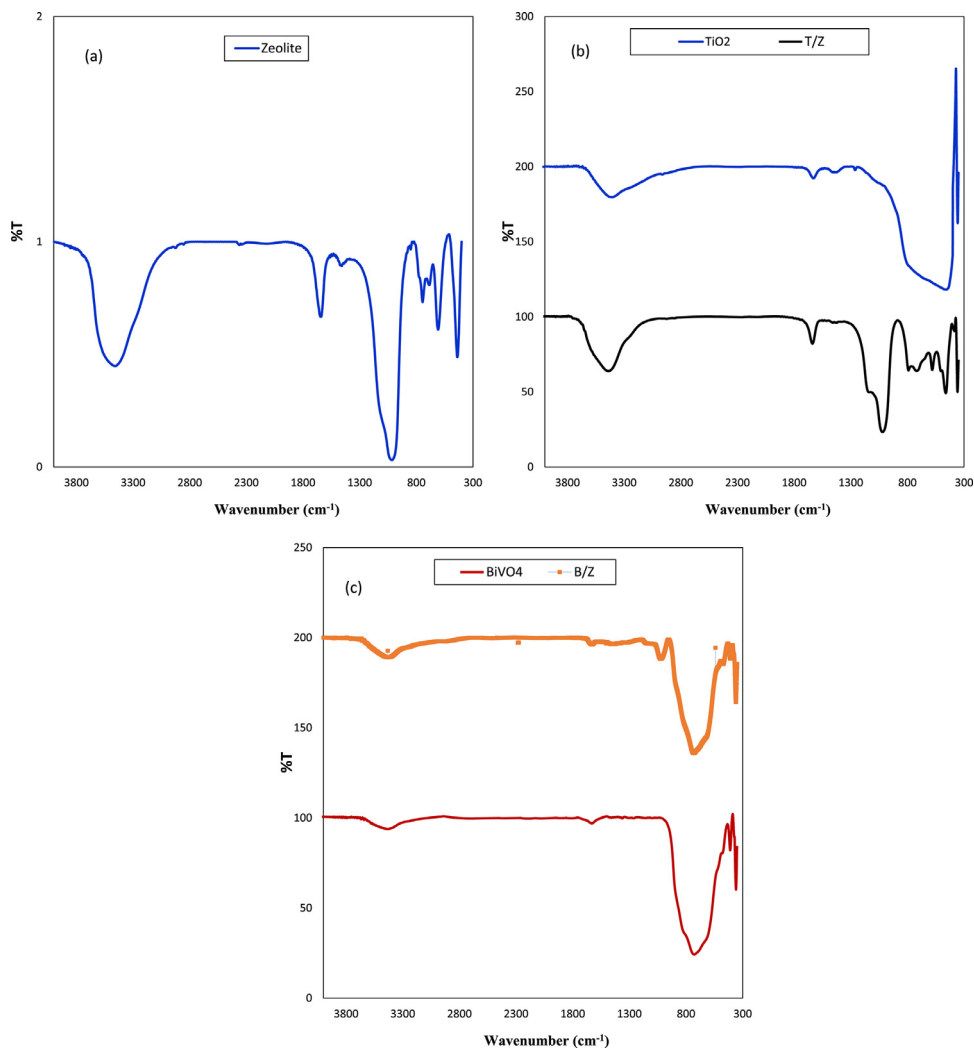


Fig. 2. The FE-SEM images of the prepared nanomaterials of a) Zeolite, b) TiO<sub>2</sub>, c) BiVO<sub>4</sub>, d) TiO<sub>2</sub>/zeolite, e) BiVO<sub>4</sub>/zeolite.

**Table 2**  
Specifications of Na-Y zeolite technical sheet.

Cation	Na
Purity (%wt.)	≥99
Na <sub>2</sub> O (%wt.)	12
Form	white powder
Shape	Sphere
Pore size (Å°)	7.5
Average particle size (μm)	0.5–1
SiO <sub>2</sub> /Al <sub>2</sub> O <sub>3</sub> (mol/mol)	6
BET surface area (m <sup>2</sup> /g)	700
Bulk density (g/mL)	0.65
Water content in package (%wt.)	≤2
Pore volume (mL/g)	0.2
X-ray crystallography (%)	95
Lattice constant (Å°)	24.39
Ignition loss (550 °C, 3 h) (%wt.)	8



**Fig. 3.** The FT-IR pattern of the studied materials of a) Zeolite b)  $\text{TiO}_2/\text{Zeolite}$ ,  $\text{TiO}_2$  c)  $\text{BiVO}_4/\text{Zeolite}$ ,  $\text{BiVO}_4$ .

software. Design response level experiments based on the coded values for dye degradation are listed in Table 5. Results of analysis of variance (ANOVA) for AO10 removal efficiency model by  $\text{TiO}_2/\text{zeolite}$  and  $\text{BiVO}_4/\text{zeolite}$  are shown in Tables 6 and 7, respectively. Parameter values of Langmuir and Freundlich isotherm results also are represented in Table 8. Correlation coefficients of pseudo-first and second order kinetic models are shown in Table 9.

## 2. Experimental Design, Materials and Methods

### 2.1. Materials and methods

Acid orange 10 dye powder, titanium dioxide (APS: 20 nm and SSA: >200  $\text{m}^2/\text{g}$ ),  $\text{Bi}(\text{NO}_3)_3 \cdot 5\text{H}_2\text{O}$ ,  $\text{NH}_4\text{VO}_3$ , Na-Y zeolite, sodium hydroxide, and hydrochloric acid were purchased

**Table 3**Studied variables and ranges for AO10 dye removal by TiO<sub>2</sub>/Zeolite composite.

Independent variables	Ranges and levels				
	-2	-1	0	+1	+2
Initial dye concentration (mg/L) (A)	10	20	30	40	50
Initial pH (B)	3	4.5	6	7.5	9
Contact time (min) (C)	1	4	7	10	13
Catalyst dosage (g/100 mL) (D)	0.05	0.1	0.15	0.2	0.25

**Table 4**Studied variables and ranges for AO10 dye removal by BiVO<sub>4</sub>/Zeolite composite.

Independent variables	Ranges and levels				
	-2	-1	0	+1	+2
Initial dye concentration (mg/L) (A)	10	20	30	40	50
Initial pH (B)	3	4.5	6	7.5	9
Contact time (min) (C)	45	90	135	180	225
Catalyst dosage (g/100 mL) (D)	0.05	0.1	0.15	0.2	0.25

**Table 5**

Design response level experiments based on coded values for dye removal.

Std	Run	A	B	C	D	Removal efficiency (%)			
						TiO <sub>2</sub> /zeolite		BiVO <sub>4</sub> /zeolite	
						Exp.	Pred.	Exp.	Pred.
8	1	1	1	1	-1	51.52	57.88	29.66	30.62
23	2	0	0	0	-2	64.87	59.92	13.94	14.97
21	3	0	0	-2	0	21.34	25.84	17.76	15.65
9	4	-1	-1	-1	1	71.09	69.52	35.76	37.58
14	5	1	-1	1	1	65.99	66.10	34.71	36.47
24	6	0	0	0	2	67.43	64.61	34.98	31.19
10	7	1	-1	-1	1	55.03	54.14	15.68	17.45
20	8	0	2	0	0	60.93	56.39	21.72	21.90
4	9	1	1	-1	-1	45.97	40.55	14.05	15.97
3	10	-1	1	-1	-1	36.44	41.11	18.09	19.11
12	11	1	1	-1	1	41.84	39.69	15.37	21.97
17	12	-2	0	0	0	99.95	88.86	59.91	57.14
2	13	1	-1	-1	-1	51.05	51.69	15.89	17.10
18	14	2	0	0	0	44.91	48.23	31.82	33.33
15	15	-1	1	1	1	81.23	85.37	50.13	51.70
7	16	-1	1	1	-1	79.25	83.13	37.59	35.31
22	17	0	0	2	0	92.08	79.81	41.93	43.27
29	18	0	0	0	0	76.77	80.47	27.87	27.78
13	19	-1	-1	1	1	97.76	100	46.95	47.84
26	20	0	0	0	0	77.61	80.47	25.89	27.78
1	21	-1	-1	-1	-1	54.93	55.49	25.75	27.01
27	22	0	0	0	0	78.51	80.47	28.39	27.78
5	23	-1	-1	1	-1	93.68	100	34.08	35.33
6	24	1	-1	1	-1	72.07	72.12	36.97	34.18
11	25	-1	1	-1	1	48.89	51.83	31.28	33.56
25	26	0	0	0	0	79.91	80.47	25.71	27.78
30	27	0	0	0	0	82.98	80.47	27.36	27.78
16	28	1	1	1	1	46.11	48.54	38.54	36.78
19	29	0	-2	0	0	91.55	88.33	31.93	29.48
28	30	0	0	0	0	87.06	80.47	31.45	27.78

**Table 6**Results of analysis of variance (ANOVA) for AO10 dye removal efficiency model by TiO<sub>2</sub>/zeolite.

Source	Sum of squares	df	Mean square	F value	P-value Prob > F
Model	10994.94	14	785.35	16.60	< 0.0001
A	2475.99	1	2475.99	52.33	< 0.0001
B	1529.45	1	1529.45	33.33	< 0.0001
C	4369.95	1	4369.95	92.35	< 0.0001
D	33.02	1	33.02	0.69	0.4166
AB	10.48	1	10.48	0.22	0.6447
AC	609.72	1	609.72	12.89	0.0027
AD	134.04	1	134.04	2.83	0.1131
BC	9.66	1	9.66	0.20	0.6579
BD	10.97	1	10.97	0.23	0.6371
CD	71.78	1	71.78	1.52	0.2370
A <sup>2</sup>	243.97	1	243.97	5.16	0.0383
B <sup>2</sup>	113.02	1	113.02	2.39	0.1431
C <sup>2</sup>	1310.57	1	1310.57	27.70	< 0.0001
D <sup>2</sup>	568.44	1	568.44	12.01	0.0035

Lack of fit: 0.063; R<sup>2</sup>: 0.93; Adeq precision: 16.5; Std. Dev.: 6.88.**Table 7**Results of analysis of variance (ANOVA) for AO10 dye removal efficiency model by BiVO<sub>4</sub>/zeolite.

Source	Sum of squares	df	Mean square	F value	P-value Prob > F
Model	4194.40	14	299.60	40.04	< 0.0001
A	924.30	1	924.30	123.52	< 0.0001
B	87.26	1	87.26	11.53	0.0040
C	1859.97	1	1859.97	248.56	< 0.0001
D	420.17	1	420.17	56.15	< 0.0001
AB	12.57	1	12.57	1.68	0.2146
AC	76.65	1	76.65	10.24	0.0060
AD	104.45	1	104.45	13.96	0.0020
BC	62.02	1	62.02	8.29	0.0115
BD	15.05	1	15.05	2.01	0.1765
CD	3.72	1	3.72	0.49	0.4913
A <sup>2</sup>	492.47	1	492.47	65.81	< 0.0001
B <sup>2</sup>	7.49	1	7.49	1.00	0.3328
C <sup>2</sup>	7.67	1	7.67	1.03	0.3373
D <sup>2</sup>	42.10	1	42.10	5.63	0.0315

Lack of fit: 0.2192; R<sup>2</sup>: 0.97; Adeq precision: 26.61; Std. Dev.: 2.74.**Table 8**

Constant values of Langmuir and Freundlich isotherm results.

Type of composite	Isotherm model	Constant	Contact time (min)	
			4	7
TiO <sub>2</sub> /zeolite	Langmuir	K <sub>L</sub>	34.92	696.53
		Q <sub>m</sub>	21.69	17.90
		R <sup>2</sup>	0.84	0.99
	Freundlich	K <sub>f</sub>	1.05	0.031
		1/n	0.63	0.26
		R <sup>2</sup>	0.81	0.77
BiVO <sub>4</sub> /zeolite	Langmuir	K <sub>L</sub>	11.77	8.53
		Q <sub>m</sub>	4.87	10.60
		R <sup>2</sup>	0.99	0.89
	Freundlich	K <sub>f</sub>	0.71	1.11
		1/n	0.11	0.36
		R <sup>2</sup>	0.76	0.92

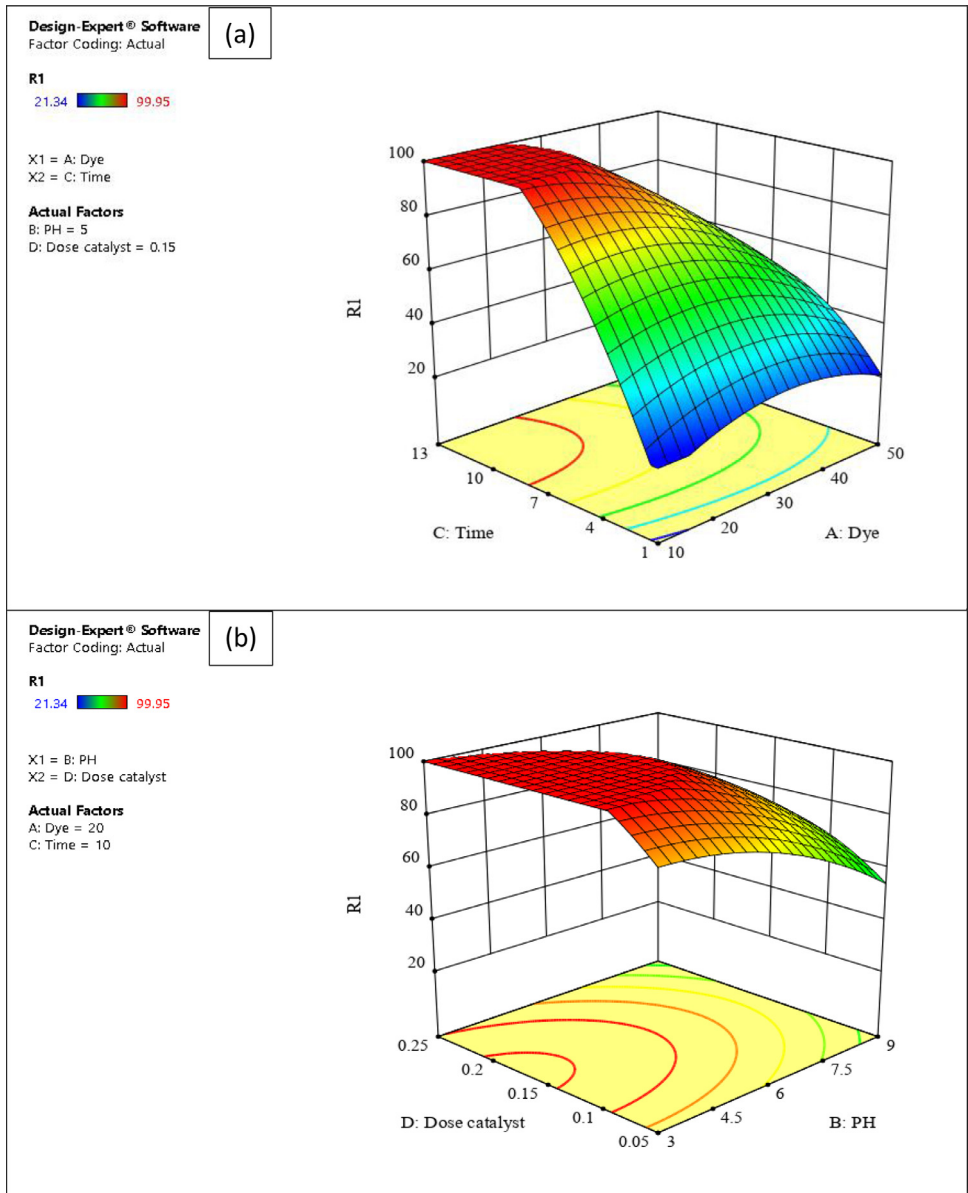


**Fig. 4.** Results of 3-D surface plots on AO10 removal efficiency for TiO<sub>2</sub> /zeolite composite of a) Time and Dye b) Dose catalyst and pH.

from Sigma Aldridge and Merck companies and were used without further purification. The removal efficiency was calculated by Eq. (1):

$$RE (\%) = \frac{C_t - C_0}{C_t} * 100 \tag{1}$$

Where C<sub>0</sub> and C<sub>t</sub> are the initial and final concentrations of dye at time = 0 and t, respectively.



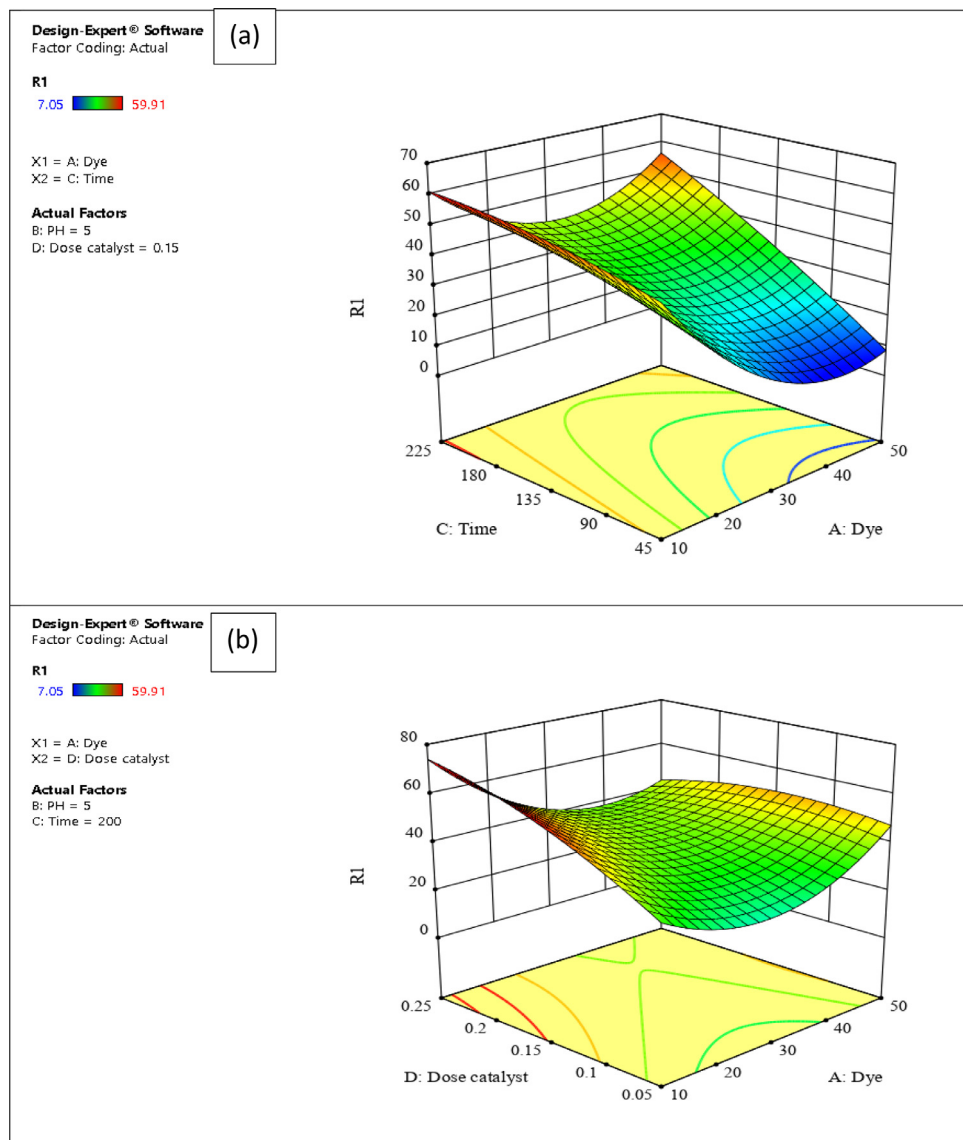


**Fig. 5.** Results of 3-D surface plots on AO10 removal efficiency for  $\text{BiVO}_4/\text{zeolite}$  composite of a) Time and Dye b) Dose catalyst and Dye.

### 2.1.1. Preparation of $\text{BiVO}_4$

In a simple and quick method, 0.02 mol of each of  $\text{Bi}(\text{NO}_3)_3 \cdot 5\text{H}_2\text{O}$ , and  $\text{NH}_4\text{VO}_3$  were dissolved in 20 mL of 4 M  $\text{HNO}_3$ , and 6 M  $\text{NaOH}$ , respectively, and stirred for 2 h at room temperature. The two solutions were mixed and stirred until a clear yellow solution was obtained. The formed slurry was then transferred to an autoclave for hydrothermal treatment and then was kept at 180 °C for 24 h. After the hydrothermal growth process, the products were washed with distilled water and ethanol and finally placed in an oven at 500 °C for 5 h [1,2].

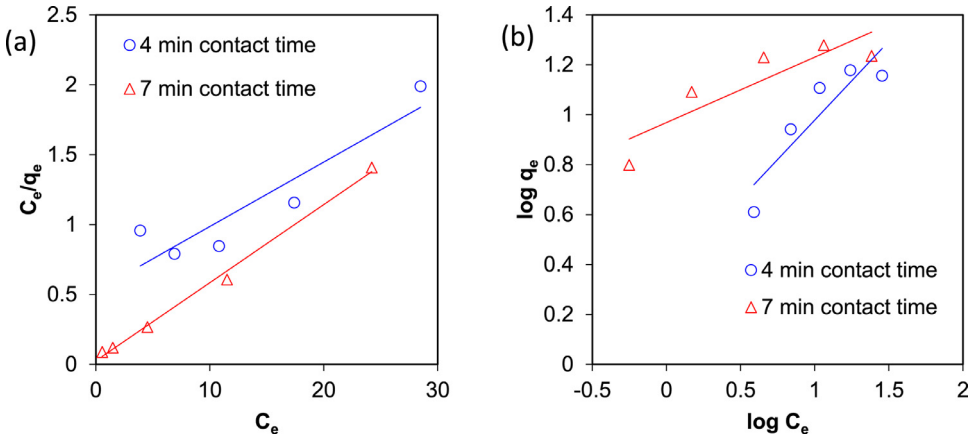


Fig. 6. Adsorption isotherms for AO10 removal on TiO<sub>2</sub>/zeolite composite of a) Langmuir and b) Freundlich.

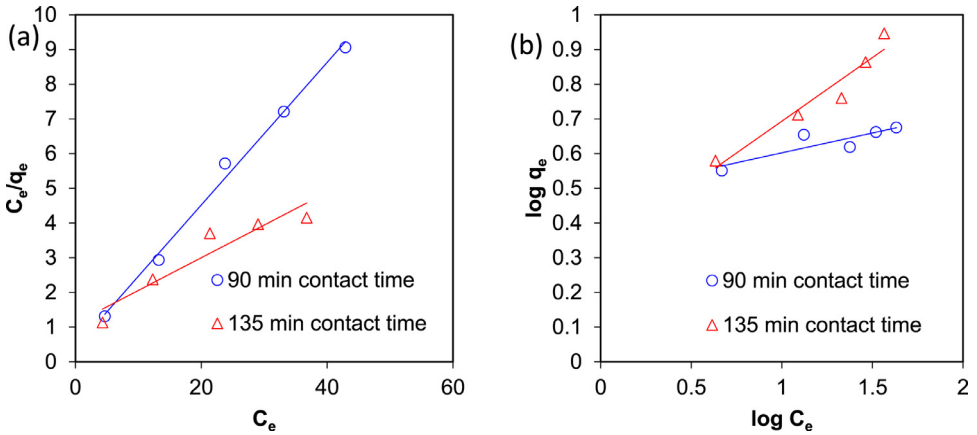


Fig. 7. Adsorption isotherms for AO10 removal on BiVO<sub>4</sub>/zeolite composite of a) Langmuir and b) Freundlich.

Table 9

Kinetic parameters for the adsorption of AO10 dye on TiO<sub>2</sub>/zeolite and BiVO<sub>4</sub>/zeolite.

Type of composite	Kinetic models	Constant	Values
TiO <sub>2</sub> /zeolite	Pseudo first-order	K <sub>1</sub>	0.107
		R <sup>2</sup>	0.84
	Pseudo second-order	K <sub>1</sub>	0.006
		R <sub>2</sub>	0.999
BiVO <sub>4</sub> /zeolite	Pseudo first-order	K <sub>1</sub>	0.003
		R <sup>2</sup>	0.89
	Pseudo second-order	K <sub>1</sub>	0.000
		R <sub>2</sub>	0.999

2.1.2. Preparation of TiO<sub>2</sub>/zeolite and BiVO<sub>4</sub>/zeolite

Here, due to the same synthesis of these two composites, both are explained together. Both composites TiO<sub>2</sub>/zeolite and BiVO<sub>4</sub>/zeolite were synthesized by the hydrothermal method, then they were mixed in equal proportions (50/50) and used in the later applications. The steps were similar to the preparation of BiVO<sub>4</sub>, except for the last step, which was placed in the oven at 400 °C for 2 h.

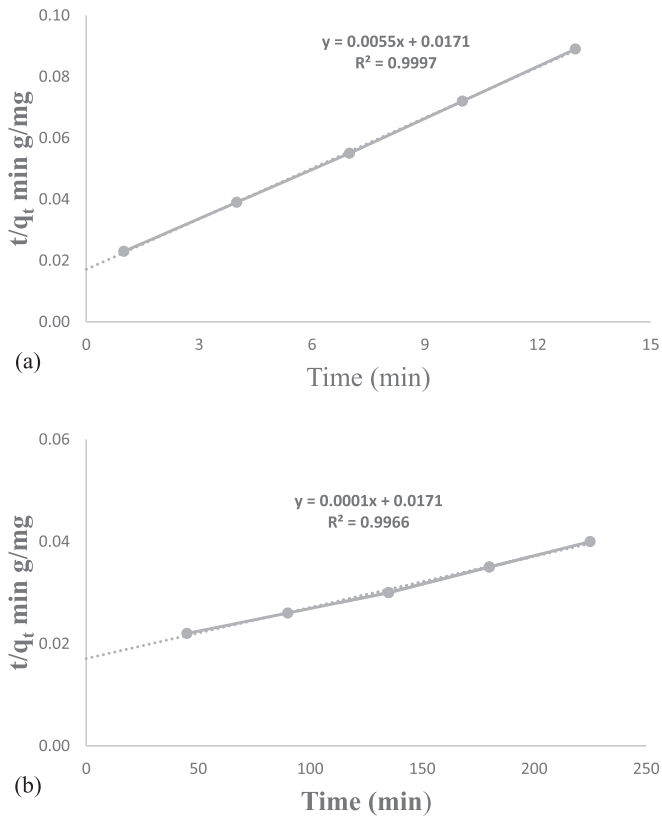


**Fig. 8.** Pseudo-second order model for nanostructure on AO10 dye removal: a)  $TiO_2/zeolite$  and b)  $BiVO_4/zeolite$ .

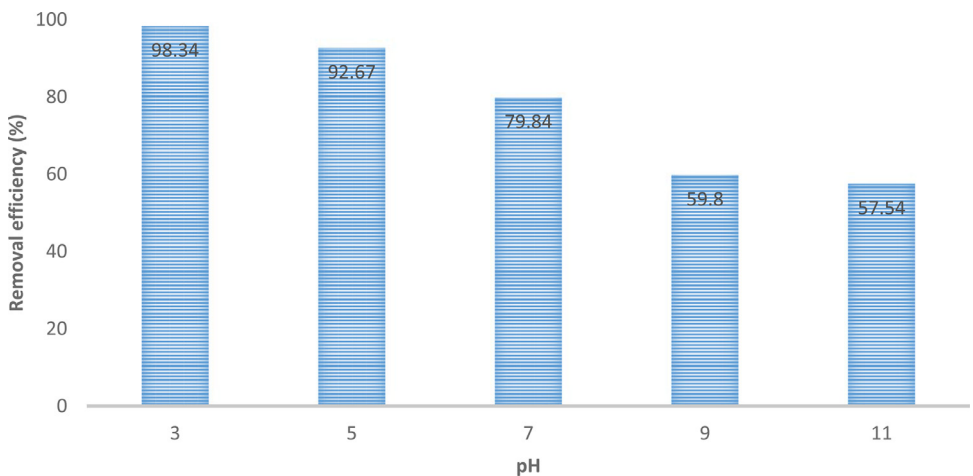


**Fig. 9.** Effect of pH on AO10 dye removal by  $TiO_2/zeolite$  nanostructure (dye concentration = 20 mg/L, contact time = 7 min, catalyst dosage = 0.2 g/100 mL).

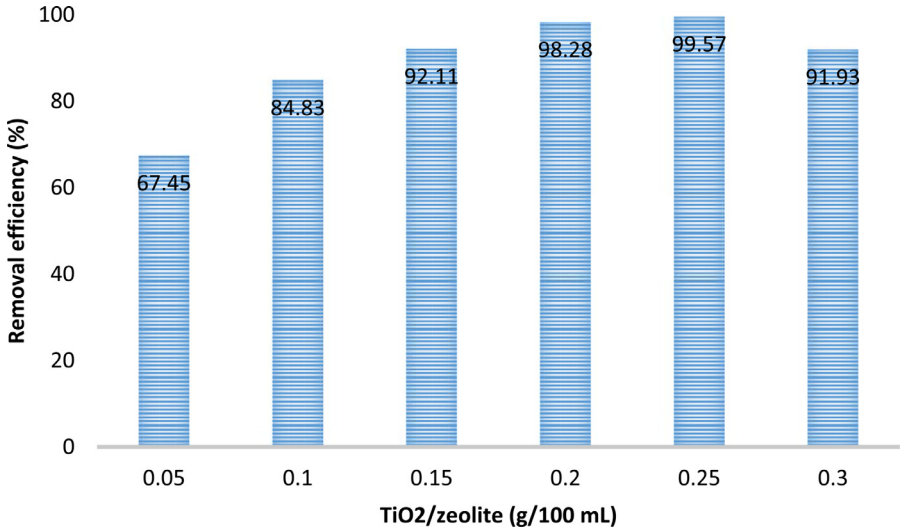


**Fig. 10.** Effect of TiO<sub>2</sub>/zeolite dosage on AO10 dye removal (dye concentration = 20 mg/L, pH = 3, contact time = 7 min.).

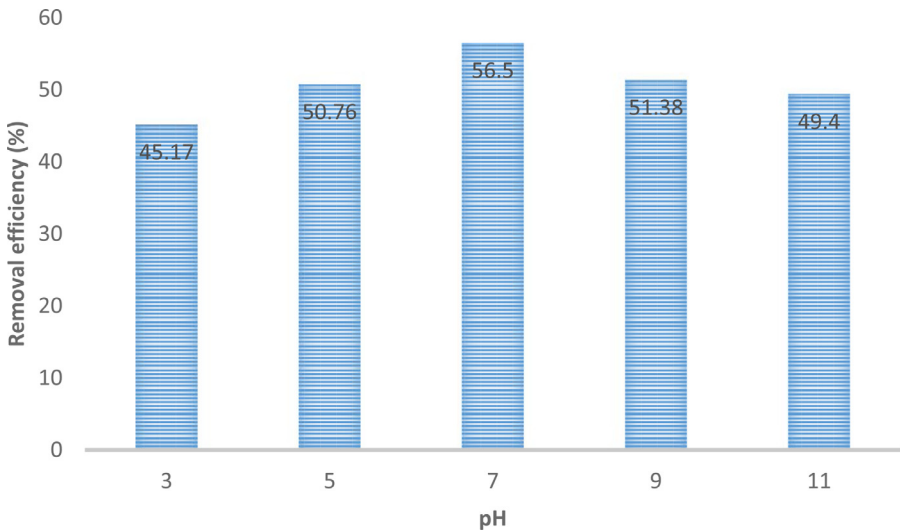


**Fig. 11.** Effect of pH on AO10 dye removal by BiVO<sub>4</sub>/zeolite nanostructure (dye concentration = 20 mg/L, Contact time = 200 min, catalyst dosage = 0.2 g/100 mL).

### 2.1.3. Nanomaterial experiments

The removal efficiency and photocatalytic oxidation experiments of AO10 solution were studied in a 100 mL pyrex glass vessel as a reactor by the investigated nanomaterials. A 125 W lamp (Philips) enclosed in a quartz casing for TiO<sub>2</sub>/zeolite immersed in the inner part of the reactor and a 12 W LED lamp (white light, light intensity = 28 mW/cm<sup>2</sup>, wavelength emission = 400–600 nm) for BiVO<sub>4</sub>/zeolite located at the top of the reaction vessel were used as light sources. The required reaction was initiated by turning on the LED and UV lamp for two systems and the samples (4 mL) were withdrawn in determined time intervals and filtered by fibreglass filter to separate nanocomposites [3].

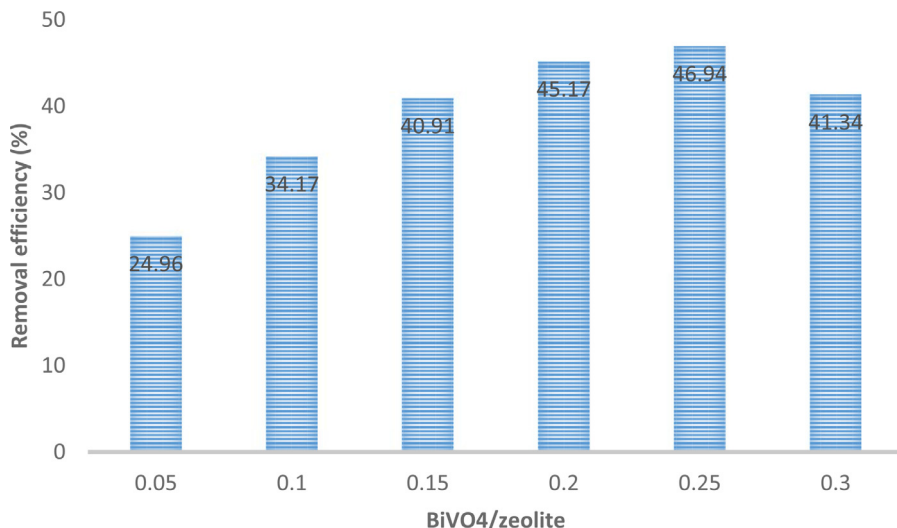


**Fig. 12.** Effect of BiVO<sub>4</sub>/zeolite dosage on AO10 dye removal (dye concentration = 20 mg/L, pH = 3, Contact time = 200 min).

## 2.2. Experimental design

In this study, an experimental design software (Design Expert ver. 11.0.1), as well the response surface methodology (RSM) were used to determine the main factors and the interaction between them and square effects, to minimize the number of experiments and save time and cost. RSM is a method dedicated to estimating the relationship between one or more response variables and some independent variables, through a set of designed experiments and regression analysis methods. The effect of initial dye concentration, pH, contact time, and catalyst dosage factors on the dye removal process at five levels was investigated. Analysis of variance (ANOVA) was used to analyze the data. The response variable is presented in the form of a polynomial regression model in Eqs. (2) and (3), for TiO<sub>2</sub>/zeolite and BiVO<sub>4</sub>/zeolite composites, respectively, which are presented as a function of independent variables.

$$Y = +80.47 - 10.16 * A - 7.98 * B + 13.49 * C + 1.17 * D + 0.8094 * AB - 6.17 * AC - 2.89 * AD - 0.7769 * BC - 0.8281 * BD - 2.12 * CD - 2.98 * A^2 - 2.03 * B^2 + 6.91 * C^2 - 4.95 * D^2 \quad (2)$$

$$Y = +27.78 - 6.21 * A - 1.90 * B + 8.80 * C + 4.18 * D - 0.8862 * AB + 2.19 * AC - 2.56 * AD + 1.97 * BC + 0.97 * BD + 0.4825 * CD + 4.24 * A^2 - 0.5227 * B^2 - 0.5290 * C^2 - 1.24 * D^2 \quad (3)$$

## 2.3. Adsorption isotherms

The linear diagrams of Langmuir and Freundlich adsorption isotherms for AO10 removal on TiO<sub>2</sub>/zeolite and BiVO<sub>4</sub>/zeolite composites are presented in Figs. 5 and 6, respectively. According to the diagrams and the values of the coefficients obtained in Table 6, it was found that the AO10 dye adsorption on both composites TiO<sub>2</sub>/zeolite and BiVO<sub>4</sub>/zeolite follows the Langmuir model.

## 2.4. Investigation of adsorption kinetics

To investigate the kinetics of AO10 dye adsorption, two kinetic models including pseudo-first order and pseudo-second order kinetic models, were used. The pseudo-second order adsorption kinetics plots for TiO<sub>2</sub>/zeolite and BiVO<sub>4</sub>/zeolite are shown in Figs. 8 and 9, respectively. The coefficients for the kinetic models can be seen in Table 9.

## 2.5. Photocatalytic mechanism of studied composites

Generally, only TiO<sub>2</sub> and BiVO<sub>4</sub> can absorb photons and be stimulated to generate electron and holes pairs. In addition, the reaction between holes and OH<sup>-</sup> and H<sub>2</sub>O adsorbed on the surface of the nanostructures particles, results in the production of OH radicals to destroy of AO10 dye. In this process, zeolite as a strong adsorbent can prevent the recombination of electron/hole pairs.

## CRedit Author Statement

**Behzad Rahimi:** Conceptualization, Investigation, Data curation, Software, Resources, Writing - Original Draft, Writing - Review & Editing; **Nayerreh Rezaie-Rahimi:** Investigation, Resources, Writing - Original Draft; **Negar Jafari:** Investigation, Resources; **Ali Abdolajnejad:** Investigation, Resources; **Afshin Ebrahimi:** Supervisor, Data curation, Resources, Idea planning, Writing - Review & Editing.

## Declaration of Competing Interest

The authors declare that they have no known competing financial interests or personal relationships that could have appeared to influence the work reported in this paper.

## Acknowledgments

The authors of this article are grateful to the Student Research Committee of Isfahan University of Medical Sciences carried out as a research project (No.196213) for supporting this project.

## Supplementary Materials

Supplementary material associated with this article can be found in the online version at <https://data.mendeley.com/datasets/v9gg6dtmzxn/1>.

## References

- [1] B. Rahimi, A. Ebrahimi, Photocatalytic process for total arsenic removal using an innovative BiVO<sub>4</sub>/TiO<sub>2</sub>/LED system from aqueous solution: optimization by response surface methodology (RSM), J. Taiwan Inst. Chem. Eng. 101 (2019) 64–79, doi:10.1016/j.jtice.2019.04.036.
- [2] B. Rahimi, N. Jafari, A. Abdolajnejad, H. Farrokhzadeh, A. Ebrahimi, Application of efficient photocatalytic process using a novel BiVO<sub>4</sub>/TiO<sub>2</sub>-NaY zeolite composite for removal of acid orange 10 dye in aqueous solutions: modeling by response surface methodology (RSM), J. Env. Chem. Eng. 7 (2019) 103253, doi:10.1016/j.jece.2019.103253.
- [3] B. Rahimi, A. Ebrahimi, N. Mansouri, N. Hosseini, Photodegradation process for the removal of acid orange 10 using titanium dioxide and bismuth vanadate from aqueous solution, Global J. Env. Sci. Manag. 5 (2019) 43–60, doi:10.22034/gjesm.2019.01.04.